**The EMBO Journal** Vol.18 No.19 pp.5166–5174, 1999

# Adhesion mechanism of human $\beta_2$-glycoprotein I to phospholipids based on its crystal structure

**Barend Bouma, Philip G.de Groot[1], Jean M.H.van den Elsen, Raimond B.G.Ravelli[2], Arie Schouten, Marleen J.A.Simmelink[1], Ronald H.W.M.Derksen[3], Jan Kroon and Piet Gros[4]**

Department of Crystal and Structural Chemistry, Bijvoet Center for Biomolecular Research, Utrecht University, Padualaan 8, 3584 CH Utrecht, [1]Haemostasis and Thrombosis Laboratory and [3]Rheumatology and Clinical Immunology, University Medical Center Utrecht, PO Box 85500, 3508 GA Utrecht, The Netherlands and [2]EMBL Grenoble Outstation, 6 Rue Jules Horowitz, B.P. 156, 38042 Grenoble Cedex 9, France

[4]Corresponding author
e-mail: p.gros@chem.uu.nl

**Human $\beta_2$-glycoprotein I is a heavily glycosylated five-domain plasma membrane-adhesion protein, which has been implicated in blood coagulation and clearance of apoptotic bodies from the circulation. It is also the key antigen in the autoimmune disease anti-phospholipid syndrome. The crystal structure of $\beta_2$-glycoprotein I isolated from human plasma reveals an elongated fish-hook-like arrangement of the globular short consensus repeat domains. Half of the C-terminal fifth domain deviates strongly from the standard fold, as observed in domains one to four. This aberrant half forms a specific phospholipid-binding site. A large patch of 14 positively charged residues provides electrostatic interactions with anionic phospholipid headgroups and an exposed membrane-insertion loop yields specificity for lipid layers. The observed spatial arrangement of the five domains suggests a functional partitioning of protein adhesion and membrane adhesion over the N- and C-terminal domains, respectively, separated by glycosylated bridging domains. Coordinates are in the Protein Data Bank (accession No. 1QUB).**

*Keywords*: anti-phospholipid antibodies/apolipoprotein H/beta2-glycoprotein I/membrane binding/short consensus repeat

## Introduction

Human $\beta_2$-glycoprotein I (β2GPI), also known as apolipoprotein H, is a membrane-adhesion glycoprotein present in blood plasma at a concentration of ~150–300 μg/ml (Willems *et al.*, 1996). It consists of 326 amino acid residues (Lozier *et al.*, 1984; Kristensen *et al.*, 1991) with ~20% w/w carbohydrates attached. β2GPI is the key antigen in the autoimmune disease anti-phospholipid syndrome (APS), defined by thrombo-embolic complications and the presence of anti-phospholipid autoantibodies (aPLs) in the blood. β2GPI has been indicated as a natural anticoagulant (Brighton *et al.*, 1996; Mori *et al.*, 1996) and has a role in the clearance of apoptotic bodies from the circulation (Price *et al.*, 1996; Balasubramanian and Schroit, 1998; Manfredi *et al.*, 1998). β2GPI belongs to a super-family of proteins characterized by repeating stretches of ~60 amino acid residues, each with a set of 16 conserved residues and two fully conserved disulfide bonds. More than 50 mammalian, mainly complement, proteins belong to this family including CR2, Factor H and CR1, which contain up to 15, 20 and 30 of these consecutive repeating stretches, respectively (Bork *et al.*, 1996). These repeating units have been termed short consensus repeat (SCR), complement control protein or Sushi domains and are, in many cases, involved in protein–protein interactions, with typically two to four consecutive domains forming an interaction site (Iwata *et al.*, 1995; Sharma *et al.*, 1996; Blom *et al.*, 1999; Casasnovas *et al.*, 1999; van de Poel *et al.*, 1999). NMR structures of two single SCR domains, domains 5 and 16 of human Factor H (HFH) (Norman *et al.*, 1991; Barlow *et al.*, 1992), and two SCR domains in tandem, domains 15–16 of HFH and domains 3–4 of vaccinia virus complement control protein (VCP) (Barlow *et al.*, 1993; Wiles *et al.*, 1997), have been determined. Recently, the crystal structure of the N-terminal two SCR domains of CD46 has been published (Casasnovas *et al.*, 1999). β2GPI consists of five of these SCR domains. The first four domains are regular SCR domains with respect to their amino acid sequences. The fifth C-terminal domain contains a six-residue insertion and a 19-residue C-terminal extension, which is C-terminally cross-linked by a disulfide bond. This aberrant domain is responsible for adhesion to acidic phospholipids (Steinkasserer *et al.*, 1992; Hunt and Krilis, 1994; Sheng *et al.*, 1996). Adhesion to membranes is very likely to be an essential aspect of β2GPI that is common to the observed effects of β2GPI in APS, coagulation and apoptosis.

The autoimmune disorder APS is characterized by the presence of a group of heterogeneous autoantibodies in blood plasma and the occurrence of thrombo-embolic complications in both the arterial and venous vasculature of patients (Bick and Baker, 1994). The symptoms appear predominantly in women aged 25–35 years. A particular problem in understanding the pathophysiology of aPLs has been the apparent contradiction between the *in vivo* observed thrombosis and the *in vitro* observed prolonged coagulation time (Brighton *et al.*, 1996). An important observation has been that the real antigen for aPLs is the plasma-protein β2GPI (Galli *et al.*, 1990) and not phospholipids (Roubey, 1996). The affinity of β2GPI for acidic phospholipids increases strongly in the presence of aPLs, which is explained by the formation of divalent $(\beta2GPI)_2$–aPL complexes (Willems *et al.*, 1996). Binding of these complexes to phospholipids interferes with the

**Table I.** Crystal characteristics showing non-isomorphism

| Crystal | Res. (Å) | m (°)[a] | *a*, *b*, *c* (Å) | ΔV/V[b] | T[c] |
|---|---|---|---|---|---|
| Native I | 29-3.75 | 1.0 | 161.53 163.73 114.99 | 0.0 | 120 |
| Native II | 40-2.7 | 1.0 | 161.17 166.49 114.51 | +1.0 | 100 |
| $K_2OsO_4$ (I) | 39-3.0 | 0.6 | 160.95 161.33 114.65 | −2.1 | 100 |
| $Na_3IrCl_6$ (I) | 38-3.1 | 0.5 | 160.55 163.11 113.98 | −1.9 | 100 |
| $K_2PtCl_6$ (I) | 39-3.2 | 0.8 | 161.38 161.86 113.98 | −2.1 | 100 |
| $K_2OsO_4$ (II) | 40-2.7 | 0.4 | 160.86 166.26 115.35 | +1.0 | 100 |
| $K_2PtCl_6$ (II) | 40-2.9 | 0.5 | 162.43 165.42 114.76 | +1.0 | 100 |

[a]Mosaicity.
[b]Native I is taken as a reference, cell volume differences are given as a percentage and are mainly caused by changes in the *b*-axis.
[c]Temperature in K during data collection.

binding of other phospholipid-binding proteins in plasma, such as coagulation proteins, resulting in the *in vitro* prolongation of coagulation (Takeya *et al.*, 1997). *In vivo*, the $(\beta 2GPI)_2$–aPL complexes possibly inhibit the anticoagulant activity of protein C at phospholipid surfaces, explaining the thrombo-embolic risk (Esmon *et al.*, 1997).

We have determined the crystal structure of the glycosylated five-domain human β2GPI purified from blood plasma to a resolution of 2.7 Å. The structure aids the characterization of the epitopes for the heterogeneous pool of aPLs and yields insights into the spatial arrangement and functional partitioning over the multiple consecutive SCR domains and the mechanism of binding to acidic phospholipids.

## Results

### Structure determination

Crystals of β2GPI grew in the orthorhombic space group $C222_1$. Significant non-isomorphism was observed between crystals, as indicated by an $R_{iso}$ of 20.9% between data sets Native I and Native II (Table I). Structure determination of β2GPI with the multiple-isomorphous replacement method using anomalous scattering (MIRAS) revealed one β2GPI molecule in the asymmetric unit with a remarkably high solvent content of 86% and a large $V_m$ value of 8.5 Å$^3$/Da (Table II, Figure 1). The initial map using Native I and derivative set I was of low quality due to poor phasing statistics (Table II) and was improved dramatically by solvent flattening using a solvent fraction of 70%. A first model was built at 3.75 Å resolution using the NMR structure of the 15th SCR domain of HFH (Barlow *et al*., 1993). Rigid-body refinement of this initial model against data set Native II yielded a decrease in *R*-factor from 52.6 to 48.0% and in $R_{free}$ from 52.0 to 47.8%. Phase information to 2.7 Å resolution obtained at a later stage (derivative sets II) was used to validate and correct the model (Figure 2). Refinement used the maximum-likelihood method and a bulk-solvent correction (see Materials and methods). Electron density corresponding to residues Ser311–Lys317 is not visible in the final $2F_o$–$F_c$ map and, therefore, these residues have not been included in the final model. Seven carbohydrate units are identified in the electron density maps at the four N-glycosylation sites. The final structure is refined to 2.7 Å resolution with an *R*-factor of 24.9% and an $R_{free}$ of 26.9% and displays good stereochemistry (Table II). Coordinates and structure factors have been deposited with the Protein Data Bank (accession No. 1QUB).

### Structure description

The structure of β2GPI shows an extended chain of five SCR domains with an overall fish-hook-like appearance with dimensions of 130 Å (vertical direction in Figure 1A), 85 Å (horizontal) and 130 Å from the N- to C-terminal extremity. The distance from the N- to C-terminal end along the curve of the molecule is ~190 Å. The fish-hook shape is mostly flat, but is bent slightly around domain III. The elongated structure contradicts a hypothetical model of Koike *et al*. (1998), who described the molecule as being folded into a compact particle.

Domains I–IV of β2GPI have common SCR folds (Figure 1B). They consist of a central anti-parallel β-sheet, comprising strands B2–B3–B4, with two extended loops typically flanked by short two-stranded anti-parallel β-sheets, B1′–B2′ and B4′–B5′, at the N- and C-terminal side (Figure 1C). Disulfide bridges located at opposite ends of a domain cross-link the short-flanking β-sheets with the central β-sheet (B1′–B4 and B3–B5′). Domain II has slightly deviating structural elements; its central sheet is extended by one more anti-parallel strand denoted B5 and residues at the position of strand B1′–B2′ do not adopt a β-sheet conformation. These four domains of β2GPI have a sequence homology ranging from 24 to 45% (Corpet, 1988) and superpose within 1.2–1.9 Å root-mean-square (r.m.s.) coordinate difference (see Materials and methods). A similar range of homology, 21–41%, and a similar range of r.m.s. coordinate difference, 1.4–2.3 Å, are observed when comparing β2GPI I–IV with SCR domains available in the Protein Data Bank, HFH-15, 16 (Barlow *et al.*, 1993) and VCP-3, 4 (Wiles *et al.*, 1997). This indicates that the SCR fold is very well conserved. The largest differences with respect to amino acid length and structure are observed in the B2–B2′ loops, referred to as 'hyper-variable' by Barlow *et al*. (1993).

The fifth C-terminal domain deviates significantly from the common SCR fold (Figure 1D). Similar to the SCR fold, it has the central anti-parallel β-sheet encompassing β-strands B2, B3 and B4 and the two disulfide bonds common to all SCR domains. In domain V, strands B3 and B4 of the central sheet are extended and are part of a larger and strongly twisted anti-parallel β-sheet. Domain V has an insertion of six residues in the region of the hyper-variable loop. This region now forms an additional β-strand (B2″), which participates in the central β-sheet, followed by a short α-helix (A1). The C-terminal extension contains a short 3/10 helix (A2) and is cross-linked C-terminally by a third disulfide bond. Residues 311–317 of this extension are not visible in the electron density map. This exposed loop is possibly mobile or disordered due to potential cleavage at Ala314–Phe315 or Lys317–Thr318 (Hunt *et al.*, 1993; Hunt and Krilis, 1994). In conclusion, domain V may be considered to consist of a core that is reminiscent of the consensus SCR fold with unique structural elements A1, A2 and B2″ and the exposed loop 311–317 forming a completely new face of this domain with respect to other known SCR domains.

**Table II.** Structure determination statistics

Diffraction data statistics[a]

| Crystal | Resolution (Å) | Redundancy | No. unique reflections | I / σ(I) | Completeness (%) | $R_{merge}$ (%)[b] |
|---|---|---|---|---|---|---|
| Native I | 29-3.75 | 4.0 | 15 447 | 5.2 (4.1) | 97.8 (97.7) | 14.7 (31.1) |
| Native II | 40-2.7 | 3.8 | 42 494 | 5.8 (2.0) | 99.8 (99.6) | 8.9 (36.3) |
| $K_2OsO_4$ (I) | 39-3.0 | 3.3 | 30 431 | 8.8 (2.6) | 96.6 (88.4) | 7.4 (28.9) |
| $Na_3IrCl_6$ (I) | 38-3.1 | 3.7 | 23 790 | 9.0 (4.4) | 83.8 (77.3) | 6.9 (20.0) |
| $K_2PtCl_6$ (I) | 39-3.2 | 3.2 | 23 516 | 8.2 (2.6) | 93.6 (67.0) | 7.8 (25.1) |
| $K_2OsO_4$ (II) | 40-2.7 | 8.9 | 42 498 | 9.7 (3.3) | 100 (99.8) | 7.4 (40.3) |
| $K_2PtCl_6$ (II) | 40-2.9 | 10.4 | 34 609 | 12.0 (5.4) | 99.5 (97.4) | 8.9 (33.1) |

Phasing statistics

| Derivative | $R_{iso}$[c] | $R_{ano}$[d] | No. sites | Phasing power[e] | | $R_{cullis}$[f] | FOM[g] |
|---|---|---|---|---|---|---|---|
| | | | | Centric | Acentric | | |
| $K_2OsO_4$ (I) | 0.230 | 0.050 | 3 | 0.65 | 0.73 | 0.67 | 0.43 |
| $Na_3IrCl_6$ (I) | 0.130 | 0.031 | 2 | 0.26 | 0.35 | 0.81 | 0.43 |
| $K_2PtCl_6$ (I) | 0.181 | 0.047 | 1 | 0.40 | 0.40 | 0.79 | 0.43 |
| $K_2OsO_4$ (II) | 0.207 | 0.063 | 4 | 0.68 | 0.76 | 0.70 | 0.34 |
| $K_2PtCl_6$ (II) | 0.213 | 0.056 | 1 | 0.47 | 0.53 | 0.76 | 0.34 |

Refinement statistics

| | |
|---|---|
| Resolution | 40-2.7 Å |
| *R*-factor/$R_{free}$[h] | 0.249/0.269 |
| r.m.s.d. bond distances | 0.019 Å |
| r.m.s.d. angles | 1.92° |
| Average B-factor | 49 Å$^2$ |
| No. non-hydrogen atoms | 2608 |
| No. protein residues | 319 |
| No. sugar moieties | 7 |
| No. solvent molecules | 32 |

[a]Numbers in parentheses indicate statistics for highest resolution shells.
[b]$R_{merge} = \Sigma_h\Sigma_i|I_{hi} - \langle I_h \rangle| / \Sigma_h\Sigma_i|I_{hi}|$
[c]$R_{iso} = \Sigma| F_{ph}^2 - F_p^2 | / | \Sigma(F_{ph}^2 + F_p^2)$
[d]$R_{ano} = \Sigma| F_{(+)}^2 - F_{(-)}^2 | / \Sigma(F_{(+)}^2 + F_{(-)}^2)$
[e]Phasing power is the r.m.s. value of the heavy atom structure factor amplitude divided by the r.m.s. residual lack of closure.
[f]$R_{cullis}$ is the mean residual lack of closure error divided by the isomorphous difference.
[g]FOM, figure of merit.
[h]A 5% test set of reflections was used for calculation of $R_{free}$.

### *Oligosaccharide antennae*

As indicated by Kristensen *et al.* (1991), human β2GPI contains four N-glycosylation sites. The electron density shows seven carbohydrate units at these four sites, namely GlcNac-α(1-*N*)-Asn143, GlcNac-α(1-*N*)-Asn164, Man-β(1–4)-GlcNac-β(1–4)-GlcNac-β(1-*N*)-Asn174 and GlcNac-β(1–4)-GlcNac-β(1-*N*)-Asn234. Weak density at Thr130 indicates the position of an O-linked sugar (Gambino *et al.*, 1997), which is in agreement with the sequence context of glycosylated threonines (Hansen *et al.*, 1995). Four glycans (at positions 130, 143, 164 and 174) are located on domain III and one (at 234) on domain IV. Three glycans are positioned in the inner curve of the fish-hook, filling the niche formed by the molecule (Figure 1A). The remaining two glycans are located on domain III at the outer curve of the fish-hook. The five glycans point into large solvent channels present in the crystal. Crystal packing is dominated by interactions involving domains I, II and V. Very few crystal contacts involve domains III and IV (Figure 3). Moreover, domains III and IV, which carry the glycans, appear to bridge between the contacts made by the N- and C-terminal domains I, II and V. The observed shielding of domains III and IV may reflect an indirect functional role of the glycans.

### *Interdomain flexibility*

The domains in β2GPI are connected by short linker regions of three (between domains IV and V) and four residues (all others), i.e. counting the number of residues between the C-terminal cysteine of the first domain and the N-terminal cysteine of the second domain. Between domains II–III and III–IV these linking residues form β-strands that connect sheets B4′–B5′ of the N-terminal domain with B1′–B2′ of the C-terminal domain (Figure 1A and B). The interactions observed at the interfaces are hydrophobic contacts with one hydrogen bond between domains I–II, II–III and III–IV and two hydrogen bonds between domains IV–V. Only a small amount (10–15%) of surface is buried at the interdomain interfaces: 422, 242, 445 and 492 Å$^2$ for domains I–II up to IV–V, respectively.

The four interdomain orientations observed in β2GPI display tilt angles (ϕ) varying from 128 to 160° and twist

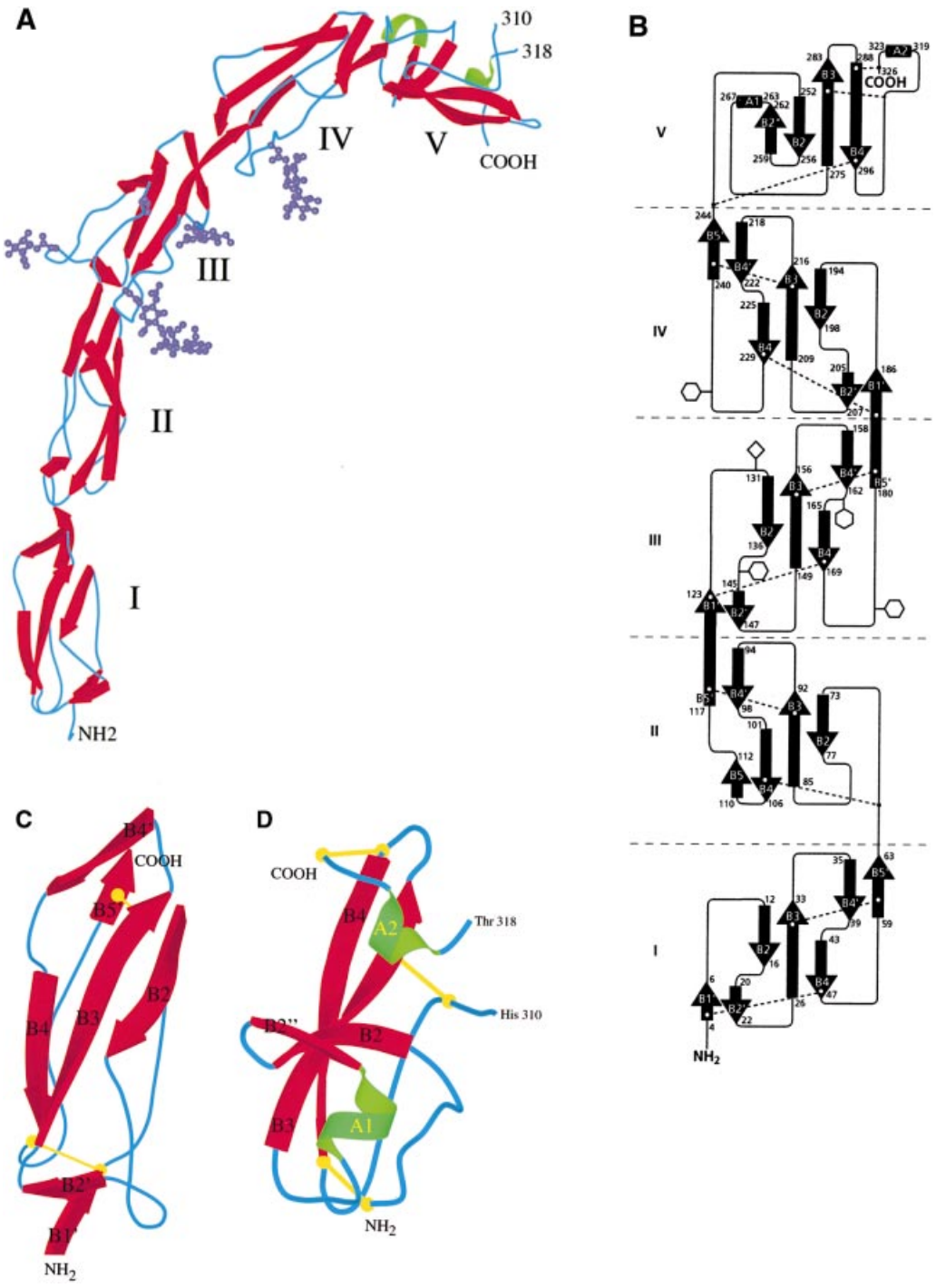


**Fig. 1.** Structural representations of human blood plasma β2GPI revealing the extended chain of the five SCR domains. (**A**) Ribbon drawing of β2GPI with consecutive domains labelled I–V. N-linked glycans, as well as the position of the putative O-linked glycan, Thr130, are indicated by a ball-and-stick model. β-strands are shown in red and helices in green. (**B**) Topology diagram of β2GPI. The central β-sheets of all five domains are labelled B2(-B2″)-B3-B4(-B5), the N- and C-terminal β-sheets are labelled B1′-B2′ and B4′-B5′, the α-helix and the 3/10 helix are denoted A1 and A2 and numbers of residues delimiting secondary structure elements are given. Disulfide bonds are indicated with dashed lines. The positions of N-glycosylation are given by hexagons; a diamond indicates the putative *O*-glycan. Horizontal dashed lines mark domain boundaries. (**C**) Ribbon representation of domain III of β2GPI with labelled secondary structure elements. The two fully conserved disulfide bonds are shown in yellow. (**D**) Ribbon representation of domain V of β2GPI with labelled secondary structure elements. The three disulfide bonds are indicated with yellow lines. The aberrant face, which contains the membrane-binding site, is located on the right-hand side.

angles (ψ) varying from 41 to 137° (Table III, Figure 4). Slightly different angles (up to 6° difference) are observed for the low-resolution data Native I, for which the *b*-axis is 2.8 Å shorter. The observed tilt angles (ϕ) in all known SCR domain–domain structures are obtuse and range from 120 to 162° (Table III). The range observed for the twist angle (ψ) is much larger, 22–180°, which indicates a large variability in precise domain–domain interactions. Electron microscopy for CR2 (Moore *et al.*, 1989) and HFH (Di Scipio, 1992), which contain 15 and 20 SCR repeats, also show elongated and winding structures. In these proteins up to eight residues link the separate

domains yielding further flexibility. These electron microscopy, NMR and X-ray data suggest that multiple SCR repeats form elongated and rather flexible chains.

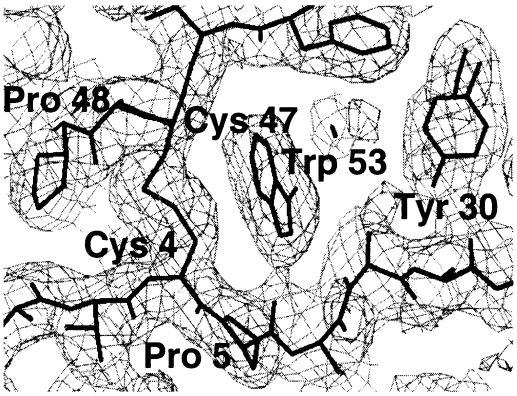


**Fig. 2.** Electron density map near Trp 53 calculated with phases from the refined model. The $2F_o$–$F_c$ map at 2.7 Å resolution is contoured at 1σ.

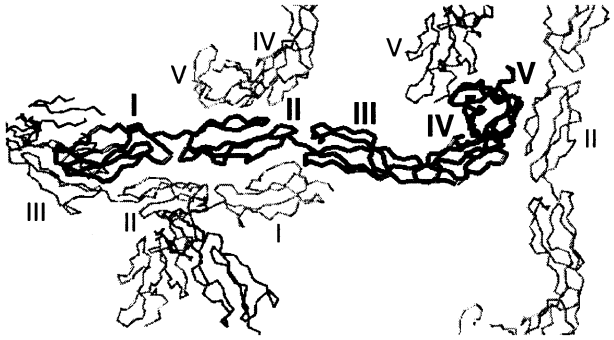


**Fig. 3.** Crystal packing of β2GPI. $C_\alpha$ traces of one molecule with its four neighbouring molecules are shown. Crystal contacts involve predominantly domains I, II and V. Contacts with glycosylated domains III and IV are restricted to the N-terminal top and C-terminal bottom of the domains III and IV, respectively. In the crystal the glycosylated domains bridge the crystal contacts made by the N- and C-terminal domains.

### *Membrane binding*

The fifth domain of β2GPI has been implicated in membrane binding (Steinkasserer *et al.*, 1992). In β2GPI we observe a large, positively charged area of ~2000 Å$^2$ on domain V (Figure 5). This patch is formed by side chains of 12 lysines, one arginine and one histidine located at the outer curve of the fish hook. It includes four lysines from the loop Cys281–Cys288 and lysines 308 and 324, which are important for phospholipid binding (Steinkasserer *et al.*, 1992; Hunt and Krilis, 1994; Sheng *et al.*, 1996). Other residues of this patch are Lys246, Lys250, Lys251, Arg260, Lys262, Lys266, Lys268 and His310. The flexible loop Ser311–Lys317, containing Trp316, which is essential for phospholipid binding (Sanghera *et al.*, 1997) is located within this charged region (Figure 5B).

The structural and biochemical data indicate a relatively simple membrane-binding mechanism. The positive charges on domain V interact with the anionic phospholipid headgroups and the flexible loop Ser311–Ser–Leu–Ala–Phe–Trp–Lys317 putatively inserts into the lipid layer and positions Trp316 at the interface region between the acyl chains and phosphate headgroups of the lipids, thereby anchoring the protein molecule to the membrane (Figure 5C). Furthermore, the combination of Trp, Phe or Tyr, followed by a Lys, is of particular importance for the interaction with the interfacial region between the lipid phosphate group and the acyl chains of lipids (Stopar *et al.*, 1996; Mall *et al.*, 1998; Mangavel *et al.*, 1998; de Planque *et al.*, 1999). Comparison of β2GPI sequences of bovine, canine, mouse, rat and human shows that the putative membrane-insertion loop Ser311–Lys317 is identical among these species and that substitutions with respect to a positively charged patch on domain V are conserved. Interestingly, all residues responsible for the unique function in membrane binding of domain V are located on the aberrant non-SCR-like half of this domain.

Reduced affinity for acidic phospholipids, as observed for the two naturally occurring mutants Cys306 to Gly and Trp316 to Ser (Sanghera *et al.*, 1997; Horbach *et al.*, 1998) and for three cleaved isoforms of β2GPI, with

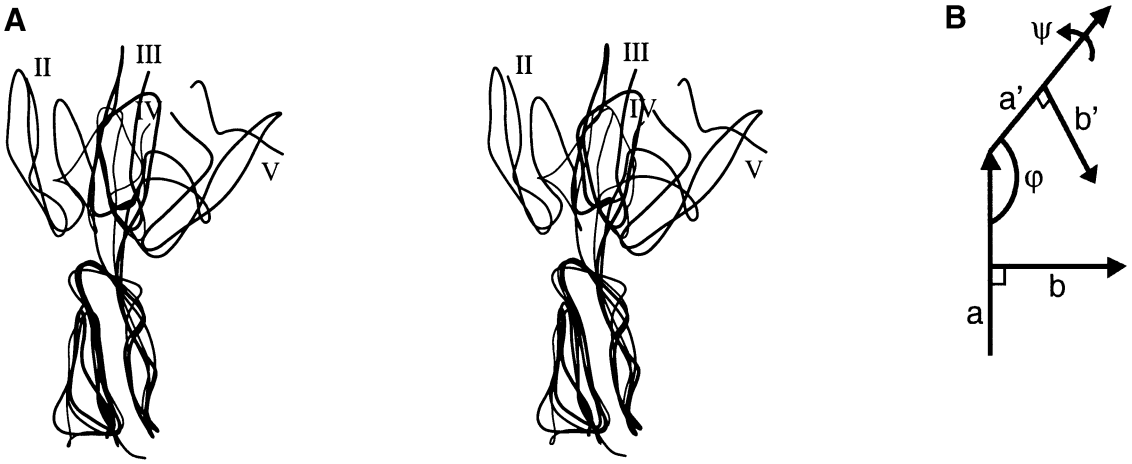


**Fig. 4.** Domain–domain orientations in β2GPI. (**A**) Stereo view of domain–domain orientations of the four sets of consecutive SCR domain pairs. The N-terminal domains of tandems II–III, III–IV and IV–V are superposed on domain I of tandem I–II. C-termini are indicated with the domain labels II–V. (**B**) The variation in domain orientations is expressed in a tilt angle ϕ and a twist angle ψ determined by the principal inertia axes *a* and *b* (Materials and methods, Table III).

**Table III.** Interdomain orientations

| | Tilt angle $\phi$ (°) | Twist angle $\psi$ (°) |
|---|---|---|
| β2GPI I–II[a] | 160, 162 | 137, 136 |
| β2GPI II–III | 160, 159 | 83, 78 |
| β2GPI III–IV | 128, 125 | 41, 46 |
| β2GPI IV–V | 131, 137 | 80, 76 |
| HFH 15–16[b] | 130 | 130 |
| CD46 1–2[c] | 120 | 180 |
| VCP 3–4[d] | 121 | 22 |

[a]Two values are given: the first value is obtained from β2GPI in crystal form II (cf. Native II), the second value refers to β2GPI in form I (Native I).
[b]Reported standard deviations are 13° in $\phi$ and 17° in $\psi$ (Wiles *et al.*, 1997).
[c]Between the six copies of the molecule in the asymmetric unit a difference of 15° in $\phi$ is reported (Casasnovas *et al.*, 1999).
[d]Reported standard deviations are 4° in $\phi$ and 6° in $\psi$ (Wiles *et al.*, 1997).

scissile bonds between residues 314–315 and 317–318 (Hunt *et al.*, 1993; Hunt and Krilis, 1994), can be readily explained by the proposed membrane-binding model. Both mutations and the two scissile bonds disrupt the integrity of the putative membrane-insertion loop 311–317. We think that the *in vitro* observed binding properties to heparin of β2GPI with the single mutation Trp316 to Ser (Horbach *et al.*, 1998), and of two isoforms that are proteolytically cleaved between Lys317 and Thr318 and native β2GPI (Horbach *et al.*, 1999), show a non-specific behaviour of the protein, which is not affected by alterations or disruptions of the membrane-insertion loop and is brought about solely by charge interactions. The loop Ser311–Ser–Leu–Ala–Phe–Trp–Lys317, therefore, gives β2GPI its specificity for phospholipid interfaces by introducing specific hydrophobic interactions between amino acid residues and acyl chains of phospholipids, in addition to the large number of charge interactions.

### *Binding of anti-phospholipid autoantibodies*

The group of autoantibodies, aPLs, detected in blood plasma of patients with APS is both inter- and intra-individually heterogeneous. Indeed, the extended shape of β2GPI offers many potential sites for antibody binding, particularly at the non-glycosylated domains I, II and V. So far, aPL binding to domains I, III, IV and V, and the interdomain region between I and II, has been reported (Hunt and Krilis, 1994; Wang *et al.*, 1995; George *et al.*, 1998; Iverson *et al.*, 1998; Blank *et al.*, 1999). Wang *et al.* (1995) have identified two potential epitope sequences, Gly274–Phe280 and Ala314–Pro325. Based on the structure, both sequences are unlikely to be epitopes of aPLs. Gly274–Phe280 forms the central β-strand B3 of domain V, which is largely inaccessible to the solvent (17% solvent accessibility). It is, thus, unlikely to be either an epitope or a cryptic epitope, without fully disrupting the fifth domain. The second peptide, Ala314–Pro325 contains part of the putative membrane-insertion loop Ser311–Lys317. Binding of aPL to these residues will directly interfere with, if not fully abolish, membrane binding of β2GPI. This analysis shows that the crystal structure of β2GPI is an important tool for the evaluation of potential epitopes. It will guide mutational studies of β2GPI and aid in the characterization of antibodies related to APS.

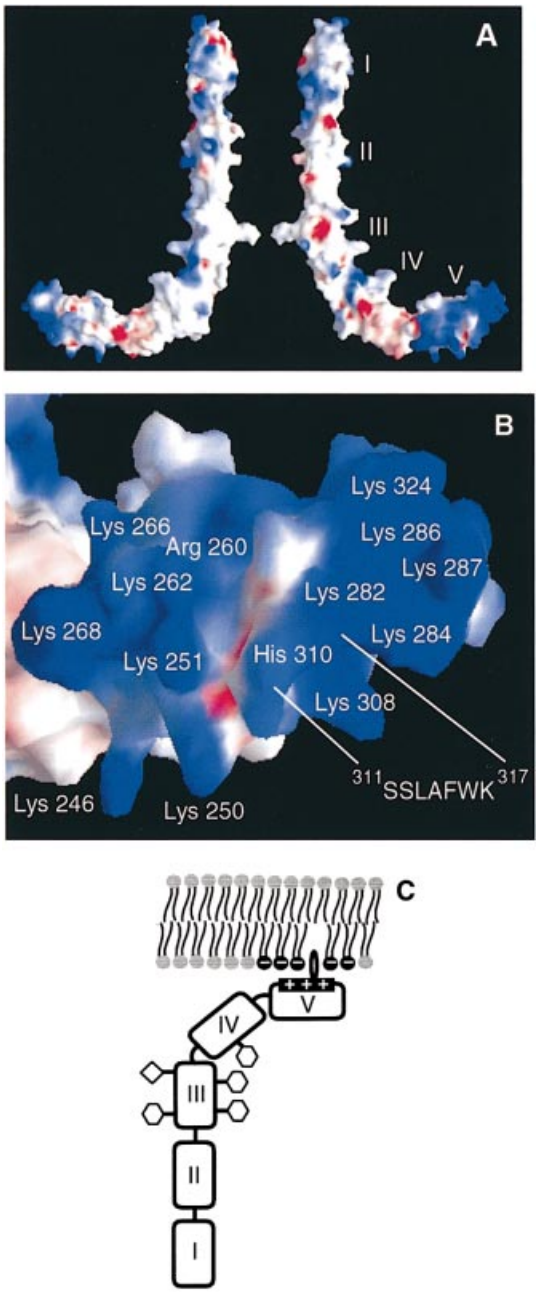


**Fig. 5.** Binding of β2GPI to an anionic phospholipid surface. (**A**) Two views, related by 180° rotation, of the electrostatic potential surface of β2GPI. Domains are labelled I–V. The electrostatic potential is scaled from red for negative to blue for positive. (**B**) Positively charged patch on the aberrant half of domain V. The 14 residues contributing to this patch and the position of the disordered loop Ser311–Lys317 are indicated. (**C**) Diagram of the proposed model for binding of β2GPI to acidic phospholipids. The positively charged patch on the surface of domain V is indicated by '+', acidic phospholipids are depicted by '–' and the putative membrane-insertion loop Ser311–Ser–Leu–Ala–Phe–Trp–Lys317 is shown to insert into the phospholipid layer. The positions of *N*-glycans are indicated by hexagons and the putative site for O-linked glycosylation is indicated by a diamond.

## Discussion

The crystal structure of the intact and glycosylated adhesion protein β2GPI from human blood plasma reveals that its five consecutive SCR domains form an elongated chain giving an overall fish-hook shape to the molecule. Multiple consecutively arranged domains are common in adhesion

molecules. However, very few structures of these repetitive domains have been resolved (Brady *et al*., 1993; Bodian *et al*., 1994; Leahy *et al.*, 1996), let alone those of complete adhesion molecules. The structure of complete β2GPI shows that the first four domains display regular SCR folds that are common to many mammalian complement proteins. The fifth domain has an aberrant fold. Constructed onto a SCR-like core, a six-residue insertion and 19-residue C-terminal extension, together with some rearrangement of existing elements, creates a completely new face on this domain. Strikingly, the structural and biochemical data strongly suggest that this new face of domain V is fully responsible for the membrane binding of β2GPI. The proposed mechanism of membrane binding consists of two major aspects: (i) a large positive patch of 14 charges binds to the anionic surface; and (ii) a flexible and partially hydrophobic loop inserts into the lipid layer and positions a Trp and a Lys at the interfacial region, thereby providing specificity for negatively charged phospholipid layers. Membrane adhesion of β2GPI probably underlies the diverse effects of this protein in blood coagulation, apoptosis and the APS immune disorder, in which autoantibodies enhance membrane affinity by divalent cross-linking of β2GPI. The observed crystal structure even bears relevance for the positioning of β2GPI domains when the molecule is membrane bound. It implies that association of the binding site, located at the top and outer curve of the fish-hook of β2GPI, with a membrane layer results in pointing domains IV to I far into the solution. Similar to what is observed in the crystal, the glycosylated domains III and IV are partially shielded from protein–protein interactions by the glycans and therefore may possibly be regarded as linker or 'bridging' domains. The N-terminal domains are exposed most to the solution and probably provide binding sites in, for example, apoptosis. Thus, the crystal structure of the complete and glycosylated adhesion molecule β2GPI suggests a functional partitioning over its three-dimensional structure that is probably a general phenomenon for many elongated multidomain adhesion molecules, as already observed, for example, in Factor H (Sharma *et al.*, 1996) and C4BP (Blom *et al.*, 1999).

## Materials and methods

### *Protein purification*

β2GPI was isolated from freshly frozen citrated human plasma of one healthy donor (Dutch Blood Bank) as described previously (Horbach *et al*., 1996). Purified β2GPI appeared as a single band of 42 kDa on an SDS–PAGE gel under non-reducing conditions and has at least seven bands between pH 5.3 and 6.8 on a silver-stained Pharmacia PhastGel IEF 3–9. MALDI-TOF mass spectrometry analysis revealed a protein mass of 45 ± 2 kDa (calculated mass 36.3 kDa), indicative of heterogeneity of the carbohydrate content and the presence of ~40–60 carbohydrate moieties. N-terminal sequence analysis revealed that this terminus starts with Gly1–Arg2–Thr3–Cys4.

### *Crystallization, heavy-atom derivatives and data collection*

Crystallization trials using the hanging-drop vapour diffusion method at 4°C were performed with β2GPI concentrated to 6.5 mg/ml in 150 mM NaCl, 50 mM Tris–HCl pH 7.3. Crystallization conditions were essentially as described by Saxena *et al.* (1998). Reservoir solutions contained either 1.5 M $(NH_4)_2SO_4$, 2% (v/v) glycerol, 20 mM $CdCl_2$ and 0.1 M HEPES pH 7.5 (Native II) or 1.5 M $(NH_4)_2HPO_4$ and 0.1 M NaOAc pH 5.6 (Native I). Large ($0.4 \times 0.4 \times 0.3$ mm$^3$) crystals of irregular shape grew within 10 days in set-ups of 1 μl protein solution and 1 μl reservoir solution. Crystals obtained under both conditions were in the orthorhombic space group $C222_1$ and were used for further experiments (Table I). Heavy-atom derivatives were prepared by soaking crystals for 4 days in solutions containing either 3 mM $K_2OsO_4$, $Na_3IrCl_6$ or $K_2PtCl_6$. Crystals were flash-frozen in a liquid nitrogen stream after equilibration in solutions with 43% (v/v) (Native I) or 30–35% (v/v) glycerol. X-ray data were collected using a Mar345 imaging plate [Hamburg, EMBL Outstation at the DESY synchrotron, beamline BW7B for data sets $K_2OsO_4$ (I), $Na_3IrCl_6$ (I) and $K_2PtCl_6$ (I)], a MacScience DIP2020 imaging plate mounted on a Nonius FR-571 rotating anode (for Native I) and an ADSC $2 \times 2$ CCD camera [Grenoble, EMBL Outstation at the ESRF synchrotron, beamline ID14-EH4 for Native II, $K_2OsO_4$ (II) and $K_2PtCl_6$ (II)]. Data collection was aided by use of STRATEGY (Ravelli *et al.*, 1997) and data were processed and scaled using either DENZO and SCALEPACK (Otwinowski and Minor, 1996) or the CCP4 Program Suite (CCP4, 1994). Unit-cell dimensions are given in Table I. Differences in cell volumes of up to 3.1% were mainly caused by differences in the length of the *b*-axis.

### *Structure determination*

Three heavy-atom derivatives were used for phasing by the MIRAS method (Table II). Heavy-atom positions were located and refined and a set of phases was calculated with SOLVE (Terwilliger and Berendzen, 1999) using data sets Native I, $K_2OsO_4$ (I), $Na_3IrCl_6$ (I) and $K_2PtCl_6$ (I). We were able to determine the presence of one β2GPI molecule in the asymmetric unit in the first electron density map phased at 3.75 Å resolution. Phases were improved by solvent flattening with a solvent fraction of 70% using the program suite CNS (Brünger *et al.*, 1998). The NMR structure of SCR domain 15 of HFH (Barlow *et al.*, 1993) was used for global positioning of the five SCR domains of β2GPI. A first model was constructed consisting of all 326 residues with 102 residues replaced by Ala. At a later stage, phase information to 2.7 Å resolution was obtained from $K_2OsO_4$ (II) and $K_2PtCl_6$ (II) using Native II (Table II). The model was validated and adjusted to the new map. The initial model was, for the most part, correct with respect to domains I–IV and contained chain-trace errors in domain V. Refinement was started with this adjusted model consisting of residues 1–131, 139–203, 210–282, 287–298 and 300–326.

### *Structure refinement*

The model was refined against the Native II data set at 2.7 Å resolution. Cycles of rebuilding using O (Jones *et al.*, 1991) and positional and B-factor refinement using model phases, using CNS, were performed until convergence. Cross-validation was used throughout the refinement. Refinement used the Maximum Likelihood algorithm (Pannu and Read, 1996) and bulk-solvent correction was applied as calculated by CNS. No electron density was visible for the loop Ser311–Lys317 in the final $2F_o$–$F_c$ electron density map, although some density indicated its position in the maps calculated with MIRAS phases at 2.7 and 3.75 Å resolution. This ill-defined, solvent-exposed region could not be modelled satisfactorily. In the vicinity of the four N-glycosylation sites, electron density was seen accounting for a total of seven carbohydrate moieties, namely GlcNac-α(1-*N*)-Asn143, GlcNac-α(1-*N*)-Asn164, Man-β(1–4)-GlcNac-β(1–4)-GlcNac-β(1-*N*)-Asn174 and GlcNac-β(1–4)-GlcNac-β(1-*N*)-Asn234, which are included in the model. No electron density accounting for fucose units linked to GlcNac-Asn was seen. The mobility of the oligosaccharide antennae is reflected by high B-factors of the carbohydrate units, ranging from 50 to 99 Å$^2$. Between Thr130 and Gly1 of a symmetry-related molecule, electron density was seen, which could possibly be ascribed to an O-linked oligosaccharide antenna attached to Thr130 (Hansen *et al.*, 1995; Gambino *et al.*, 1997). Additional electron density, which may be accounted for by cadmium ions, is observed near His172, His216 and Glu309. Near Tyr207's hydroxyl group additional weak density is present that might be indicative of partial sulfatation. Side-chain positions of residues Arg2, Arg39, Lys 59, Lys110, Arg135, Gln158, Lys177, Lys208, Lys251, Lys284, Glu285, Lys286, Lys287, Lys308 and Glu309 are poorly defined. The average B-factors for the main-chain atoms ($C_\alpha$, C, O, N) of the domains (labelled I–V) are 41.6 Å$^2$ (I), 38.1 Å$^2$ (II), 52.7 Å$^2$ (III), 53.8 Å$^2$ (IV) and 57.9 Å$^2$ (V), with an average B-factor for all domains of 46.9 Å$^2$. For all non hydrogen protein atoms (i.e. excluding glycans) the B-factors are 42.1 Å$^2$ (I), 39.3 Å$^2$ (II), 53.8 Å$^2$ (III), 54.8 Å$^2$ (IV) and 59.2 Å$^2$ (V), with an average B-factor for all domains of 48.0 Å$^2$. The final model comprises β2GPI residues Gly1–His310, residues Thr318–Cys326, one mannose and six *N*-acetylglucosamine carbohydrate moieties, which accounts for ~80% of the total mass of a β2GPI molecule and 32 ordered water molecules.

### *Crystal structure analysis*

Superpositions of SCR domains are calculated in O using first cysteine residues only, followed by superpositioning of $C_\alpha$ positions of spatially related residues (distance cut-off 3.8 Å). R.m.s. coordinate differences of 1.2–2.3 Å are observed for superposing 39 to 59 residues of β2GPI domains I–IV, HFH domains 15, 16 and VCP domains 3, 4. Domain–domain orientations of β2GPI were calculated using 27 $C_\alpha$ atoms from each domain, which superposed with r.m.s. coordinate differences of 1.17–1.50 Å, as calculated with O. All domains were translated to one origin and for each domain inertia tensors were calculated and diagonalized. One domain was rotated with respect to its preceding domain in such a way that their eigenvectors with the smallest eigenvalues, i.e. the main axes of the domains (labelled a and a′ in Figure 4B), were aligned (tilt angle φ). Next, a second rotation (twist angle ψ) was performed to align the eigenvectors (labelled b and b′ in Figure 4B) with the second-smallest eigenvalues. Definition of the tilt angle φ and twist angle ψ is according to Bork *et al.* (1996). Molecular surfaces and electrostatic potentials were calculated using GRASP (Nicholls *et al.*, 1993). The model quality was checked using WHATIF (Vriend, 1990) and PROCHECK (Laskowski *et al.*, 1993). The Ramachandran plot for the final model comprising 319 amino acid residues, shows that 87.4% of these residues fall in the most favoured region with no residues in disallowed regions. Domain–domain contacts were calculated with LIGPLOT (Wallace *et al.*, 1995). Figures 1A, C, D and 4A were generated using MOLSCRIPT (Kraulis, 1991).

## Acknowledgements

We thank Professor A.Heck (Department of Mass Spectrometry, Utrecht), Mr F.van der Lecq (Sequence Centre Utrecht), Mrs B.Lutters, Drs D.A.Horbach and A.B.M.Linssen for assistance, and Professor A.T.Brünger (Yale University, CT) and Dr T.K.Sixma (Netherlands Cancer Institute, Amsterdam, The Netherlands) for critically reading the manuscript. We also thank the staff of the EMBL Outstation at DESY (Hamburg, Germany) for assistance in X-ray data collection and the European Union for support of the work at EMBL (Hamburg, Germany) through the HCMP Access to Large Installations Project, contract number CHGE-CT-0040. We thank Dr S.McSweeney of the EMBL Grenoble Outstation for data collection at the ESRF beam-line ID14-EH4. R.B.G.R. acknowledges support from the TMR Access to Large Scale Facilities contract ERBFMGECT980133 to the EMBL Grenoble Outstation. M.J.A.S. is supported by a grant from the Dutch League against Rheumatism (97-1-401). This research was financially supported by the Council for Chemical Sciences of the Netherlands Organization for Scientific Research.

## References

Balasubramanian,K. and Schroit,A.J. (1998) Characterization of phosphatidylserine dependent $\beta_2$-glycoprotein I macrophage interactions. *J. Biol. Chem.*, **273**, 29272–29277.

Barlow,P.N., Norman,D.G., Steinkasser,A., Horne,T.J., Pearce,J., Driscoll,P.C., Sim,R.B. and Campbell,I.D. (1992) Solution structure of the fifth repeat of factor H: a second example of the complement control protein module. *Biochemistry*, **31**, 3626–3634.

Barlow,P.N., Steinkasser,A., Norman,D.G., Kieffer,B., Wiles,A.P., Sim,R.B. and Campbell,I.D. (1993) Solution structure of a pair of complement modules by nuclear magnetic resonance. *J. Mol. Biol.*, **232**, 268–284.

Bick,R.L. and Baker,W.F. (1994) Antiphospholipid and thrombosis syndromes. *Semin. Thromb. Hemost.*, **20**, 3–15.

Blank,M., Shoenfeld,Y., Cabilly,S., Heldman,Y., Fridkin,M. and Katchalski-Katzir,E. (1999) Prevention of experimental antiphospholipid syndrome and endothelial cell activation by synthetic peptides. *Proc. Natl Acad. Sci. USA*, **96**, 5164–5168.

Blom,A.M., Webb,J., Villoutreix,B.O. and Dahlbäck,B. (1999) A cluster of positively charged amino acids in the C4BP α-chain is crucial for C4b binding and Factor I cofactor function. *J. Biol. Chem.*, **274**, 19237–19245.

Bodian,D.L., Jones,E.Y., Harlos,K., Stuart,D.I. and Davis,S.J. (1994) Crystal structure of the extracellular region of the human cell adhesion molecule CD2 at 2.5 Å resolution. *Structure*, **2**, 755–766.

Bork,P., Downing,K.A., Kieffer,B. and Campbell,I.D. (1996) Structure and distribution of modules in extracellular proteins. *Q. Rev. Biophys.*, **29**, 119–167.

Brady,R.L., Dodson,E.J., Dodson,G.G., Lange,G., Davis,S.J., Williams, A.F. and Barclay,A.N. (1993) Crystal structure of domains 3 and 4 of rat CD4: relation to the $NH_2$-terminal domains. *Science*, **260**, 979–983.

Brighton,T.A., Hogg,P.J., Dai,Y.-P., Murray,B.H., Chong,B.H. and Chesterman,C.N. (1996) $\beta_2$-glycoprotein I in thrombosis: evidence for a role as a natural anticoagulant. *Br. J. Haematol*, **93**, 185–194.

Brünger,A.T. *et al.* (1998) Crystallography and NMR system: a new software suite for macromolecular structure determination. *Acta Crystallogr. D*, **54**, 905–921.

Casasnovas,J.M., Larvie,M. and Stehle,T. (1999) Crystal structure of two CD46 domains reveals an extended measles virus-binding surface. *EMBO J.*, **18**, 2911–2922.

CCP4 (1994) The CCP4 suite: programs for protein crystallography. *Acta Crystallogr. D*, **50**, 760–763.

Corpet,F. (1988) Multiple sequence alignment with hierarchical clustering. *Nucleic Acids Res.*, **16**, 10881–10890.

de Planque,M.R.R., Kruijtzer,J.A.W., Liskamp,R.M.J., Marsh,D., Greathouse,D.V., Koeppe,R.E., de Kruijff,B. and Killian,J.A. (1999) Different membrane anchoring positions of tryptophan and lysine in synthetic transmembrane α-helical peptides. *J. Biol. Chem.*, **274**, 20839–20847.

Di Scipio,R.G. (1992) Ultrastructures and interactions of complement factors H and I. *J. Immunol.*, **149**, 2592–2599.

Esmon,N.L., Smirnov,M.D. and Esmon,C.T. (1997) Thrombogenic mechanisms of antiphospholipid antibodies. *Thromb. Haemost.*, **78**, 79–82.

Galli,M., Comfurius,P., Maassen,C., Hemker,H.C., de Baets,M.H., van Breda-Vriesman,P.J.C., Barbui,T., Zwaal,R.F.A. and Bevers,E.M. (1990) Anticardiolipin antibodies (ACA) directed not to cardiolipin but to a plasma protein cofactor. *Lancet*, **335**, 1544–1547.

Gambino,R., Ruiu,G., Pagano,G. and Cassader,M. (1997) Qualitative analysis of the carbohydrate composition of apolipoprotein H. *J. Protein Chem.*, **16**, 205–212.

George,J., Gilburd,B., Hojnik,M., Levy,Y., Langevitz,P., Matsuura,E., Koike,T. and Shoenfeld,Y. (1998) Target recognition of $\beta_2$-glycoprotein I ($\beta_2$GPI)-dependent anticardiolipin antibodies: evidence for involvement of the fourth domain of $\beta_2$GPI in antibody binding. *J. Immunol.*, **160**, 3917–3923.

Hansen,J.E., Lund,O., Engelbrecht,J., Bohr,H., Nielsen,J.O., Hansen, J.E.S. and Brunak,S. (1995) Prediction of O-glycosylation of mammalian proteins: specificity patterns of UDP-GalNac:polypeptide *N*-acetylgalactosaminyltransferase. *Biochem. J.*, **308**, 801–813.

Horbach,D.A., van Oort,E., Donders,R.C.J.M., Derksen,R.H.W.M. and de Groot,P.G. (1996) Lupus anticoagulant is the strongest risk factor for both venous and arterial thrombosis in patients with systematic lupus erythematosus—comparison between different assays for detection of antiphospholipid antibodies. *Thromb. Haemost.*, **76**, 916–924.

Horbach,D.A., van Oort,E., Tempelman,M.J., Derksen,R.H.W.M. and de Groot,P.G. (1998) The prevalence of a non-phospholipid-binding form of $\beta_2$-glycoprotein I in human plasma. *Thromb. Haemost.*, **80**, 791–798.

Horbach,D.A., van Oort,E., Lisman,T., Meijers,J.C., Derksen, R.H.W.M. and de Groot,P.G. (1999) $\beta_2$-glycoprotein I is proteolytically cleaved *in vivo* upon activation of fibrinolysis. *Thromb. Haemost.*, **81**, 87–95.

Hunt,J.E. and Krilis,S.A. (1994) The fifth domain of $\beta_2$-glycoprotein I contains a phospholipid binding site (Cys281-Cys288) and a region recognized by anticardiolipin antibodies. *J. Immunol.*, **152**, 653–659.

Hunt,J.E., Simpson,R.J. and Krilis,S.A. (1993) Identification of a region of $\beta_2$-glycoprotein I critical for lipid binding and anti-cardiolipin antibody cofactor activity. *Proc. Natl Acad. Sci. USA*, **90**, 2141–2145.

Iverson,G.M., Victoria,E.J. and Marquis,D.M. (1998) Anti-β2 glycoprotein I (β2GPI) autoantibodies recognize an epitope on the first domain of β2GPI. *Proc. Natl Acad. Sci. USA*, **195**, 15542–15546.

Iwata,K., Seya,T., Yanagi,Y., Pesando,J.M., Johnson,P.M., Okabe,M., Ueda,S., Ariga,H. and Nagasawa,S. (1995) Diversity of sites for measles virus binding and for inactivation of complement C3b and C4b on membrane cofactor protein CD46. *J. Biol. Chem.*, **270**, 15148–15152.

Jones,T.A., Zou,J.Y., Cowan,S.W. and Kjeldgaard,M. (1991) Improved methods for the building of protein models in electron density maps and the location of errors in these models. *Acta Crystallogr. A*, **47**, 110–119.

Koike,T., Ichikawa,K., Kasahara,H., Atsumi,T., Tsutsumi,A. and Matsuura,E. (1998) Epitopes on β2-GPI recognized by anticardiolipin antibodies. *Lupus*, **7 (***Suppl. 2*), 14–17.

Kraulis,P. (1991) Molscript: a program to produce both detailed and schematic plots of protein structures. *J. Appl. Crystallogr.*, **24**, 946–950.

Kristensen,T., Schousboe,I., Boel,E., Mulvihill,E.M., Rosendahl

Hansen,R., Bach Møller,K., Hundahl Møller,N.P. and Sottrup-Jensen,L. (1991) Molecular cloning and mammalian expression of human $\beta_2$-glycoprotein I cDNA. *FEBS Lett.*, **289**, 183–186.

Laskowski,R.A., MacArthur,M.W., Moss,D.S. and Thornton,J.M. (1993) PROCHECK—a program to check the stereochemical quality of protein structures. *J. Appl. Crystallogr.*, **26**, 283–291.

Leahy,D.J., Aukhil,I. and Erickson,H.P. (1996) 2.0 Å crystal structure of a four-domain segment of human fibronectin encompassing the RGD loop and synergy region. *Cell*, **84**, 155–164.

Lozier,J., Takahashi,N. and Putnam,F.W. (1984) Complete amino acid sequence of human plasma $\beta_2$-glycoprotein I. *Proc. Natl Acad. Sci. USA*, **81**, 3640–3644.

Mall,S., Sharma,R.P., East,J.M. and Lee,A.G. (1998) Lipid–protein interactions in the membrane: studies with model peptides. *Faraday Discuss.*, **111**, 127–136.

Manfredi,A.A., Rovere,P., Heltai,S., Galati,G., Nebbia,G., Tincani,A., Balestrieri,G. and Sabbadini,M.G. (1998) Apoptotic cell clearance in systematic lupus erythematosus II. Role of $\beta_2$-glycoprotein I. *Arthritis Rheum.*, **41**, 215–223.

Mangavel,C., Maget-Dana,R., Tauc,P., Brochon,J.C., Sy,D. and Reynaud,J.A. (1998) Structural investigations of basic amphipathic model peptides in the presence of lipid vesicles studied by circular dichroism, fluorescence, monolayer and modeling. *Biochim. Biophys. Acta*, **1371**, 265–283.

Moore,M.D., DiScipio,R.G., Cooper,N.R. and Nemarrow,G.R. (1989) Hydrodynamic electron microscopic and ligand-binding analysis of the Epstein–Barr virus/C3dg receptor (CR2). *J. Biol. Chem.*, **264**, 20576–20582.

Mori,T., Takeya,H., Nishioka,J., Gabazza,E.C. and Suzuki,K. (1996) $\beta_2$-Glycoprotein I modulates the anticoagulant activity of activated protein C on the phospholipid surface. *Thromb. Haemost.*, **75**, 49–55.

Nicholls,A., Sharp,K.A. and Honig,B. (1993) GRASP: graphical representation and analysis of surface properties. *Biophys. J.*, **64**, 166–170.

Norman,D.G., Barlow,P.N., Baron,M. Day,A.J., Sim,R.B. and Campbell,I.D. (1991) Three dimensional structure of a complement control protein module in solution. *J. Mol. Biol.*, **219**, 717–725.

Otwinowski,Z. and Minor,W. (1996) Processing of X-ray diffraction data collected in oscillation mode. *Methods Enzymol.*, **276**, 307–326.

Pannu,N.S. and Read,R.J. (1996) Improved structure refinement through Maximum Likelihood. *Acta Crystallogr. A*, **52**, 659–668.

Price,B.E. *et al*. (1996) Antiphospholipid autoantibodies bind to apoptotic, but not viable, thymocytes in a $\beta_2$-glycoprotein I-dependent manner. *J. Immunol.*, **157**, 2201–2208.

Ravelli,R.B.G., Sweet,R.M., Skinner,J.M., Duisenberg,A.J.M. and Kroon,J. (1997) STRATEGY: a program to optimize the starting spindle angle and scan range for X-ray data collection. *J. Appl. Crystallogr.*, **30**, 551–554.

Roubey,R.A.S. (1996) Immunology of the antiphospholipid antibody syndrome. *Arthritis Rheum.*, **39**, 1444–1454.

Sanghera,D.K., Wagenknecht,D.R., McIntyre,J.A. and Kamboh,M.I. (1997) Identification of structural mutations in the fifth domain of apolipoprotein H ($\beta_2$-glycoprotein I) which affect phospholipid binding. *Hum. Mol. Genet.*, **6**, 311–316.

Saxena,A., Gries,A., Schwarzenbacher,R., Kostner,G.M., Laggner,P. and Prassl,R. (1998) Crystallization and preliminary X-ray crystallographic studies on apolipoprotein H (β2 glycoprotein-I) from human plasma. *Acta Crystallogr. D*, **54**, 1450–1452.

Sharma,A.K. and Pangburn,M.K. (1996) Identification of three physically and functionally distinct binding sites for C3b in human complement factor H by deletion mutagenesis. *Proc. Natl Aacd. Sci. USA*, **93**, 10996–11001.

Sheng,Y., Sali,A., Herzog,H., Lahnstein,J. and Krilis,S.A. (1996) Site-directed mutagenesis of recombinant human $\beta_2$-glycoprotein I identifies a cluster of lysine residues that are critical for phospholipid binding and anti-cardiolipin antibody activity. *J. Immunol.*, **157**, 3744–3751.

Steinkasserer,A., Barlow,P.N., Willis,A.C., Kertesz,Z., Campbell,I.D., Sim,R.B. and Norman,D.G. (1992) Activity, disulfide mapping and structural modelling of the fifth domain of human $\beta_2$-glycoprotein I. *FEBS Lett.*, **313**, 193–197.

Stopar,D., Spruijt,R.B., Wolfs,C.J. and Hemminga,M.A. (1996) Local dynamics of the M13 major coat protein in different membrane-mimicking systems. *Biochemistry*, **35**, 15467–15473.

Takeya,H., Mori,T., Gabazza,E.C., Kuroda,K., Deguchi,H., Matsuura,E., Ichkawa,K., Koike,T. and Suzuki,K. (1997) Anti-β2-glycoprotein I (β2GPI) monoclonal antibodies with lupus anticoagulant-like activity enhance the β2GPI binding to phospholipids. *J. Clin. Invest.*, **99**, 2260–2268.

Terwilliger,T.C. and Berendzen,J. (1999) Automated MAD and MIR structure solution. *Acta Crystallogr. D*, **55**, 849–861.

Van der Poel,R.H.L., Meijers,J.C.M. and Bouma,B.N. (1999) Interaction between protein S and complement C4b-binding protein (C4BP). *J. Biol. Chem.*, **274**, 15144–15150.

Vriend,G. (1990) WHAT IF: A molecular modelling and drug design program. *J. Mol. Graph.*, **8**, 52–56.

Wallace,A.C., Laskowski,R.A. and Thornton,J.H. (1995) LIGPLOT: a program to generate schematic diagrams of protein–ligand interactions. *Protein Eng.*, **8**, 127–134.

Wang,M.X., Kandiah,D.A., Ichikawa,K., Khamashta,M., Hughes,G., Koike,T., Roubey,R. and Krilis,S.A. (1995) Epitope specificity of monoclonal anti-$\beta_2$ glycoprotein I antibodies derived from patients with the antiphospholipid syndrome. *J. Immunol.*, **155**, 1629–1636.

Wiles,A.P., Shaw,G., Bright,J., Perczel,A., Campbell,I.D. and Barlow,P.N. (1997) NMR studies of a viral protein that mimics the regulators of complement activation. *J. Mol. Biol.*, **272**, 253–265.

Willems,G.M., Janssen,M.P., Pelsers,M.M., Comfurius,P., Galli,M., Zwaal,R.F. and Bevers,E.M. (1996) Role of divalency in the high-affinity binding of anticardiolipin antibody β2-glycoprotein I complexes to lipid membranes. *Biochemistry*, **35**, 13833–13842.

*Received June 21, 1999; revised and accepted August 2, 1999*